JOC The Journal of Organic Chemistry

Article

pubs.acs.org/joc

Natural Bond−Bond Polarizability: A Hückel-Like Electronic Delocalization Index

H. E. Zimmerman† and F. Weinhold*

Department of Chemistry and Theoretical Chemistry Institute, University of Wisconsin, Madison, Wisconsin 53706, United States

ABSTRACT: We show how the bond−bond polarizability index, as originally introduced by Coulson and Longuet−Higgins in the Hückel-theoretic context, can be generalized in the natural bond orbital (NBO) framework to ab initio molecular orbital and density functional theory levels. We demonstrate that such a "natural bond−bond polarizability" (NBBP) index provides a flexible and quantitative descriptor for a broad spectrum of delocalization effects ranging from strong π aromaticity to weak intra- and intermolecular hyperconjugative phenomena. Illustrative applications are presented for representative delocalization effects in saturated and unsaturated species, chemical reactions, and hydrogen-bonding interactions.

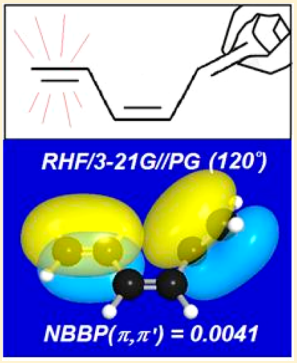

INTRODUCTION

Coulson and Longuet−Higgins[1] originally introduced the concept of bond−bond polarizability $\Pi_{b;b'}$ in their classic molecular orbital (MO) treatment of π-electron systems. If $\pi_b = 2^{-1/2}[p_r + p_s]$ is a normalized π bond between p-orbitals on atoms r, s, and $\pi_{b'} = 2^{-1/2}[p_t + p_u]$ similarly between atoms t, u, the bond−bond polarizability can be written as

$$\Pi_{b;b'} = \Pi_{rs;tu} = 2 \sum_{j(occ)} \sum_{k(vir)} (c_{rj}c_{sk} + c_{rk}c_{sj})(c_{tj}c_{uk} + c_{tk}c_{uj}) / (\varepsilon_k - \varepsilon_j) \quad (1)$$

where c_{rj} and c_{rk}, respectively, denote the LCAO coefficients of p_r in an occupied (φ_j) or virtual (φ_k) π MO and ε_j and ε_k are the corresponding orbital energies.

In the Hückel framework, $\Pi_{b;b'}$ can be expressed as

$$\Pi_{b;b'} = \Pi_{rs;tu} = \partial P_{rs}/\partial\beta_{tu} = \frac{1}{2}\partial^2 E/\partial\beta_{rs}\partial\beta_{tu} = \Pi_{tu;rs} \quad (2)$$

where P_{rs} is the r−s π bond order (off-diagonal density matrix element) and β_{tu} the off-diagonal Hückel matrix element between p_t and p_u. Equation 2 identifies the physical significance of $\Pi_{b;b'}$, which measures how the r−s bond order is affected by changes in the off-diagonal Hückel matrix element β_{tu} (due, e.g., to changes in t−u interatomic distance or other perturbations[2]). Colloquially speaking, $\Pi_{b;b'}$ predicts how loudly bond b "squeals" if bond b′ is "pinched".

Equations 1 and 2 were obtained with the usual Hückel π-electron orthogonality assumption, $\langle p_r \mid p_s\rangle = \delta_{rs}$. Chirgwin and Coulson[3] developed a generalized expression that includes overlap corrections, and McWeeny[4] discussed possible self-consistent generalizations for such Hückel-type formulas (cf. Greenwood and Hayward[5]). In the intermediate neglect of differential overlap (INDO) approximation, Pople and Santry[6] developed well-known approximations for nuclear spin coupling constants that incorporate the related "atom−atom polarizability" index ($\Pi_{rr;ss}$). However, little use has been made of $\Pi_{rs;tu}$ in the framework of modern ab initio molecular orbital (MO) and density functional theory (DFT).

The arguments leading to eqs 1, 2 can be applied virtually without modification in the framework of natural bond orbital (NBO) analysis of ab initio wave functions.[7] Each localized bond NBO b is expressed in terms of natural hybrid orbitals (NHOs) h_r, h_s and associated polarization coefficients a_r, a_s,

$$b = b_{rs} = a_r h_r + a_s h_s \quad (3)$$

that satisfy Hückel-like orthonormality relations

$$\langle h_r | h_s\rangle = \delta_{rs} \quad (4a)$$

$$\langle b | b\rangle = a_r^{\,2} + a_s^{\,2} = 1 \quad (4b)$$

In this case, the β_{rs} parameter can be identified as the r−s Fock or Kohn−Sham matrix element between NHOs h_r and h_s

$$\beta_{rs} = (\mathbf{F})_{rs} = \langle h_r | F_{op} | h_s\rangle \quad (5)$$

but the formulas are otherwise unmodified. Whereas the original Hückel treatment reflects only topological (graph-theoretic connectivity) aspects of carbon planar π networks, eq 5 incorporates the quantitative dependencies on geometry, electronegativity differences, and other chemically significant variables. Equations 1 and 2 can be applied to describe σ and π bond−bond polarizability in arbitrary molecular systems for which ab initio MO/DFT densities and corresponding NBOs have been obtained. We refer to the $\Pi_{rs;tu}$ defined by eqs 1−5 as

Special Issue: Howard Zimmerman Memorial Issue

Received: July 31, 2012
Published: August 22, 2012

Table 1. Bond−Bond Polarizability ($\Pi_{rs;tu}$) Values for *trans*-Butadiene, Showing Comparison of HMO and ab Initio Values at Various Theory Levels[a]

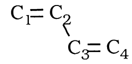

method	$\Pi_{1,2;1,2}$	$\Pi_{1,2;2,3}$	$\Pi_{1,2;2,4}$	$\Pi_{1,2;3,4}$	$\Pi_{2,3;2,3}$
Hückel theory[b]	0.306	−0.615		0.306	1.231
RHF/STO-3G (R=1.4)	0.2101	−0.5409	−0.0021	0.2100	1.3934
RHF/STO-3G (PG)	0.1337	−0.5322	−0.0414	0.1334	1.3858
RHF/3-21G (PG)	0.1694	−0.6477	−0.0336	0.1684	1.5271
RHF/6-31G* (PG)	0.1664	−0.6411	−0.0400	0.1643	1.5200
B3LYP/6-31G* (PG)	0.4466 [0.201][c]	−1.1032 [−0.496][c]	0.0205 [0.009][c]	0.4448 [0.200][c]	2.7376 [1.231][c]

[a]Results are given for two idealized geometries: an equivalent-bonds model (R = 1.4: $R_{12} = R_{23} = R_{34}$ = 1.40 Å) and a near-experimental Pople−Gordon model ("PG": $R_{12} = R_{34}$ = 1.34 Å, R_{23} = 1.46 Å), both with idealized 120° valence angles. [b]Analytic HMO results in units of inverse β (Streitwieser, ref 2, p 108), evaluated with $\beta = -0.2909$ to match the corresponding RHF/STO-3G (R = 1.4) Fock matrix element $F_{1,2}$ for π-bonded p_1−p_2 orbitals. [c]Rescaled β to match the HMO value to the B3LYP value for the largest HMO element ($\Pi_{2,3;2,3}$).

Table 2. π Bond−bond Polarizabilities for Styrene (See Text for Atomic Labels), Comparing Hückel Values (in Parentheses; Taken from Streitweiser, Ref 2) with ab Initio NBBP Values (RHF/6-31G*//PG level)[a]

bond	π_{12}	π_{34}	π_{56}	π_{ab}
π_{12}	0.997 (0.987)	0.495 (0.487)	0.467 (0.444)	0.092 (0.174)
π_{34}	0.495 (0.487)	1.003 (1.003)[a]	0.508 (0.503)	0.007 (0.036)
π_{56}	0.467 (0.444)	0.508 (0.503)	0.980 (0.987)	−0.031 (−0.044)
π_{ab}	0.092 (0.174)	0.007 (0.036)	−0.031 (−0.044)	0.153 (0.289)

[a]Adjusted to NBBP value, $\beta = -0.252$. [a]The Hückel parameter $\beta = -0.252$ was chosen to equate the largest element ($\prod_{34;34}$) for the two methods.

the "natural bond−bond polarizability" (NBBP) to suggest its heritage in NBO-based generalization of the delocalization descriptor as first introduced by Coulson and Longuet-Higgins.

In limiting cases, the NBBP index can be related to other NBO measures of electronic delocalization. As shown in the Appendix, when electrons are delocalized from bond σ_{rs} to antibond σ^*_{tu}, $\Pi_{rs;tu}$ is approximately proportional to the corresponding second-order NBO interaction energy $\Delta E^{(2)}_{\sigma(rs)\sigma^*(tu)}$

$$\Pi_{rs;tu} \propto \Delta E^{(2)}_{\sigma(rs)\sigma^*(tu)} \qquad (6)$$

which is routinely provided in NBO energetic analysis of MO wave functions. However, the NBBP index $\Pi_{rs;tu}$ includes simultaneous effects of $\sigma_{rs}\rightarrow\sigma^*_{tu}$ and $\sigma_{tu}\rightarrow\sigma^*_{rs}$ delocalization (or other general interactions) and has a more familiar connection to Hückel-type concepts than do the perturbative $\Delta E^{(2)}_{\sigma(rs)\sigma^*(tu)}$ quantities.

The goal of this work is to present illustrations of NBBP indices for classic cases of π and σ conjugation. We thereby seek to document the general applicability to modern ab initio MO wave function technology, preservation of elementary Hückel-like concepts, and numerical robustness with respect to variations of theory level and chemical complexity. These illustrative applications complement more specific NBBP investigations in systems of mechanistic and photochemical interest.[8] The NBBP index also complements other NBO-based extensions of qualitative bonding concepts, including through-bonds superexchange pathways,[9] Fukui functions,[10] Hammett-type relationships,[11] or other aspects of Hückel-like conjugation and cross-conjugation.[12]

Illustrative NBBP Applications. In the present work, we employ a standard Gaussian[13] host program linked to the NBO5-level analysis module[14] to evaluate NBBP indices for familiar MO/DFT theoretical levels.[15]

π Delocalization in Butadiene, Benzene, and Styrene. Table 1 presents an elementary application of the ab initio NBBP method to the π system of *trans*-butadiene, illustrating the comparison with the classic Hückel (HMO) treatment. To make a direct comparison with HMO theory, we first employ an unrealistic model geometry with equal CC bond lengths, R_{CC} = 1.40 Å (corresponding to the single fixed β of HMO theory) and minimal STO-3G basis set, as shown in the first two rows of Table 1. In all cases we employ the "sign-corrected" $\Pi_{rs;tu}$ values of NBBP output[14] for consistent fixed-β comparisons with HMO theory.

As the comparisons of Table 1 show, the Hückel BBP values differ somewhat from ab initio NBBP values, but an overall pattern of qualitative agreement can be recognized. The third row of Table 1 shows the corresponding RHF/STO-3G NBBP values for more realistic Pople−Gordon[16] (PG) geometry with unequal CC bond lengths. The agreement with standard HMO fixed-β values, although somewhat reduced, is still qualitatively reasonable. The fourth and fifth rows of Table 1 exhibit corresponding values for split-valence 3-21G and polarized double-ζ 6-31G* basis sets, illustrating the usual strong convergence characteristics of NBO-based descriptors as the basis set extends toward compleness. Finally, the sixth row shows corresponding DFT (B3LYP/6-31G*) values that exhibit the significant overall enhancement of conjugative delocalization due to dynamical electron correlation. The bracketed values of the final row show how a more direct comparison with the HMO indices can be achieved by adjusting β to match a particular HMO value to the corresponding calculated DFT value (e.g., for the largest NBBP element), as will also be done in the following examples. In the ensuing examples we also make consistent use of idealized PG geometry in order to emphasize that the subtle stereochemical variations of $\Pi_{rs;tu}$ (and resulting changes in optimized geometry) reflect intrinsic electronic *causes* (rather

than indirect *consequences*) of subtle variations in nuclear geometry.

Whereas the Hückel treatment cannot distinguish *trans* (*anti*) and *cis* (*syn*) geometries, the ab initio NBBP indices reveal somewhat stronger delocalization effects in the *trans* rotamer. For example, at RHF/6-31G*//PG level the diagonal ($\prod_{12;12}$) and off-diagonal ($\prod_{12;34}$) π–π polarizabilities for *trans*-butadiene (0.1664, 0.1643) are appreciably higher than those for *cis*-butadiene (0.1365, 0.1354), reflecting the general conjugative preference for *trans* open-chain geometry. One can also compare these values with the corresponding values for benzene (1.0032, 0.5200; RHF/6-31G*//PG) to recognize that the π NBBP index is significantly stronger in the latter case, in accordance with the higher degree of delocalization associated with cylic aromatic conjugation.

As an additional representative example of aromatic species, we present in Table 2 a comparison of HMO and ab initio NBBP values for styrene (RHF/6-31G*//PG), with corresponding atomic labels as shown:Since the ab initio $\langle \pi | F_{op} | \pi' \rangle$

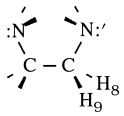

values are all distinct in this case, we can choose a particular β value (= −0.252) to match the largest NBBP element to the corresponding HMO value. Table 2 shows that the HMO and NBBP values are again in excellent agreement within the aromatic ring. The discrepancies are somewhat larger for the exocyclic π_{ab} bond (cf. Table 1, where the HMO values are similarly too large compared to ab initio counterparts), but overall agreement is again quite reasonable. Figure 1 graphically illustrates the high correlation (correlation coefficient r = 0.993) between ab initio and semiempirical $\Pi_{b;b'}$ values for this case. The general consistency with previous values for the exocyclic vinyl group (cf. Table 1) and aromatic ring system (cf.

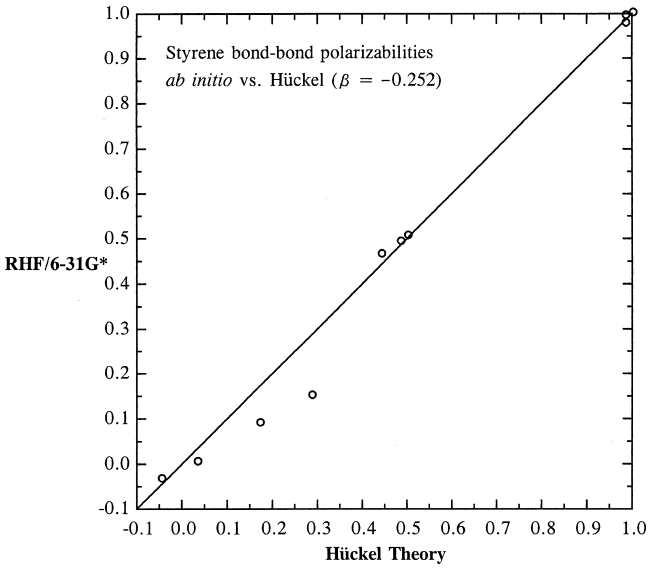

Figure 1. Comparison of ab initio (RHF/6-31G* level, idealized Pople–Gordon geometry) and Hückel theory (β = −0.252) π-bond polarizabilities for styrene, showing the high correlation (r = 0.993) of ab initio NBBP indices with semiempirical Hückel values. Cf. Table 2 for identification of individual values.

benzene results quoted above) also indicates the reasonable transferability of $\Pi_{rs;tu}$ elements, consistent with chemical intuition.

π and σ Delocalization in Twisted Hexatriene. Figure 2 illustrates a related application to hexatriene (RHF/6-31G*//

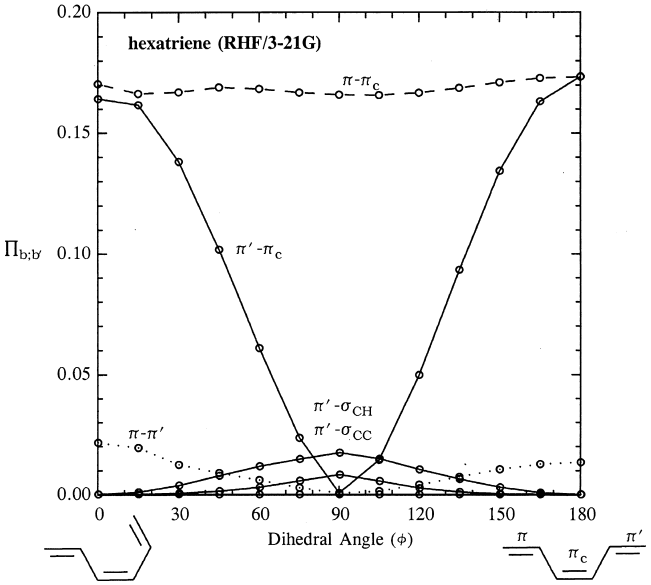

Figure 2. Natural bond–bond polarizability index $\Pi_{b;b'}$ for selected NBOs b, b′ of hexatriene (RHF/3-21G level, idealized Pople–Gordon geometry, with π-bond labels identified at lower right) showing the dependence on twisting about the single bond to π'. Conjugative interactions are shown for the untwisted π (dashed lines) and twisted π' (solid lines) bonds with vicinal σ_{CC}, σ_{CH}, or central π_c and with each other (dotted line).

PG level) in which one of the π bonds is twisted about a CC single bond to demonstrate the strong dependence of π-delocalization on conformation. As this figure illustrates, the NBBP index for the π_c–π' interaction drops sharply for the π bonds twisted out of planarity, whereas the untwisted π–π_c interaction retains the essentially constant value (~0.17) characteristic of *trans*-butadiene. This is in accord with well-known torsional dependencies of π conjugation, which lie outside the topological Hückel framework.

Figure 2 also shows the dramatically different strengths of nearest-neighbor (π_c–π') vs next-nearest-neighbor (π–π') π-type NBBP elements, emphasizing the essentially *local* (vicinal) character of strong conjugative π–π interactions. The small magnitudes of nonvicinal π–π' NBBP elements can be judged from the feeble overlap of π- and π'-type NBOs, as depicted in the PNBO[17] overlap diagram of Figure 3 for dihedral angle φ = 120°. The near-zero π–π' overlap in Figure 3 correctly suggests the small π–π' NBBP value ($\Pi_{\pi-\pi'}$ = 0.0041), comparable to the conjugative π'-σ_{CC} value at the same geometry. Pi-conjugation can indeed lead to "long range" delocalization effects, but such effects are generally achieved through a succession of local vicinal "relays" rather than direct interaction of remote isolated π bonds, despite the impression that is sometimes conveyed by the superficial "delocalization" of canonical MOs.[18]

Figure 2 also illustrates the non-zero NBBP values between the twisted π' bond and the σ framework (vicinal σ_{CC} and σ_{CH} bonds), reflecting a hyperconjugative π–σ delocalization effect that arises when σ–π symmetry is broken. Figure 2 illustrates

dx.doi.org/10.1021/jo301620k | J. Org. Chem. 2013, 78, 1844–1850

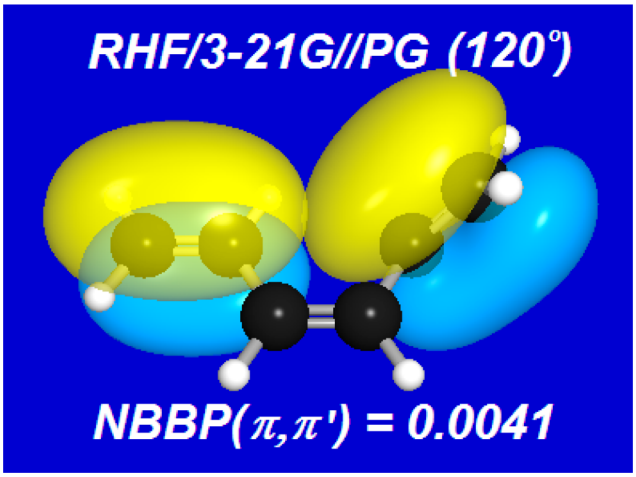

Figure 3. Pre-NBO (PNBO) overlap diagram for nonvicinal $\pi-\pi'$ interactions in hexatriene at φ = 120° (cf. Figure 2), showing the characteristically weak orbital overlap that corresponds to feeble NBBP value ($\Pi_{\pi;\pi'}$ = 0.0041) for nonadjacent π bonds.

how conjugative and hyperconjugative delocalization effects are simultaneously described by the NBBP matrix in a unified manner for arbitrary nonplanar arrangements.

Sigma Delocalization in 1,2-Diaminoethane. To further illustrate the qualitative parallels (despite wide disparities in strength) between σ and π delocalization effects, we consider the evaluation of $\Pi_{rs;tu}$ for the saturated 1,2-diaminoethane molecule (RHF/6-31G*//PG level), as shown in Figure 4 (with key atomic labels identified in the figure caption). The initial φ = 180° geometry corresponds to NCCN linkages in diaza[2.2.2]bicyclooctane (DABCO), with both lone pairs lying *anti* to the CC bond. As either amino group twists about a CN bond, one observes (Figure 4) the strong angular variations of $n_N'-\sigma_{CC}$ interaction between the amine lone pair and the central σ_{CC} bond, qualitatively similar to the conjugative $\pi'-\pi_c$ interactions of Figure 2. The weaker delocalization effects of saturated species can be identified as "secondary hyperconjugation" in the terminology of Mulliken[19] or "negative hyperconjugation" in that of Schleyer and Kos[20] (for a comprehensive recent review, see ref 21). The NBBP values are in accord with numerous experimental and theoretical studies of long-range "through-bond" interactions in DABCO and related systems.[22]

In Figure 4 one can see the vivid oscillations of hyperconjugative $n'-\sigma_{CH}$ interactions with vicinal CH bonds as the lone pair swings successively into coplanar alignments with these bonds. As the relative amplitudes of the $\Pi_{n'-\sigma}$ indicate, these hyperconjugative interactions are strongest in *anti*periplanar arrangements, in accordance with the known pattern of β-elimination and other stereoelectronic effects involving lone pairs.[23] The greater strength of $\Pi_{n'-\sigma}$ in *anti* (staggered) vs *syn* (eclipsed) conformations is also consistent with the general hyperconjugative picture of the origin of internal rotation barriers[24] and related anomeric phenomena.

Intermolecular π Delocalization in a Model Diels–Alder Reaction. The NBBP index can also be used to exhibit π delocalization effects in *inter*molecular interactions. As an example, we investigate the potential barrier for a symmetric model Diels–Alder 4 + 2 cycloaddition reaction between *cis*-butadiene and ethylene (RHF/3-21G level)[25]

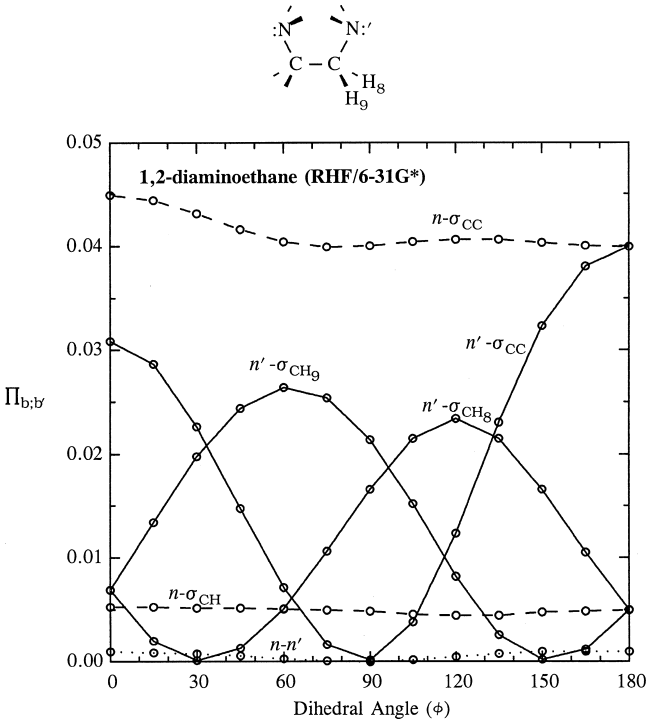

Figure 4. Natural bond–bond polarizability index $\Pi_{b;b'}$ for selected NBOs b, b' of 1,2-diaminoethane (RHF/6-31G*//PG) showing the dependence on twisting about the C–N′ amino bond (φ = CCNn' dihedral angle). The displayed curves depict hyperconjugative interactions of amine lone pairs n (untwisted; dashed lines), n' (twisted; solid lines) with vicinal CC or CH bonds, or with one another (dotted line). Note that conjugative $\Pi_{n'-\sigma}$ interactions are maximal at angles 0° (σ_{CC}), 60° (σ_{CH8}), or 120° (σ_{CH9}) where σ bonds come into coplanar alignment with the amine lone pair (stronger in *anti*, weaker in *syn* conformation).

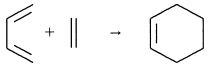

as shown in Figure 5 (with key atomic labels identified in the figure caption). The reaction coordinate R_{rc} is taken as the distance from the ethylene (dienophile) CC bond midpoint to a point midway between terminal C atoms of the diene. Other coordinates are optimized at each value of R_{rc}, subject to preserving C_s symmetry and CCCC planarity.

Figure 5 shows the calculated energy profile (solid line, right-hand ordinate) along R_c in the range from 1.43 Å (equilibrium product species, cyclohexene) to 3.0 Å (weakly interacting reactant species, ethylene + butadiene, slightly inside van der Waals contact distance). Consistent with the known experimental failure of ethylene and butadiene to undergo appreciable Diels–Alder reaction except under activating conditions, the calculated potential energy profile in this case exhibits a rather high barrier (~30 kcal/mol) along the reactant channel.[26] An apparent exponential increase[27] of intermolecular π'(ethylene)–π_b(butadiene) delocalization is evident as the reactant species approach the transition state at $R_{rc}^{\ddagger}$ = 2.09 Å. The calculated NBBP values clearly reflect the powerful $\pi'-\pi^*$ delocalizations between the filled ethylene π-bond and unfilled π^* antibonds of the diene ("HOMO–LUMO interactions"), in accordance with the familiar picture of [4 + 2] cycloaddition reactions.[28] As shown in Figure 5, other intermolecular $\Pi_{b;b'}$ elements are so weak as to be negligible in the reactant regime.

dx.doi.org/10.1021/jo301620k | J. Org. Chem. 2013, 78, 1844–1850

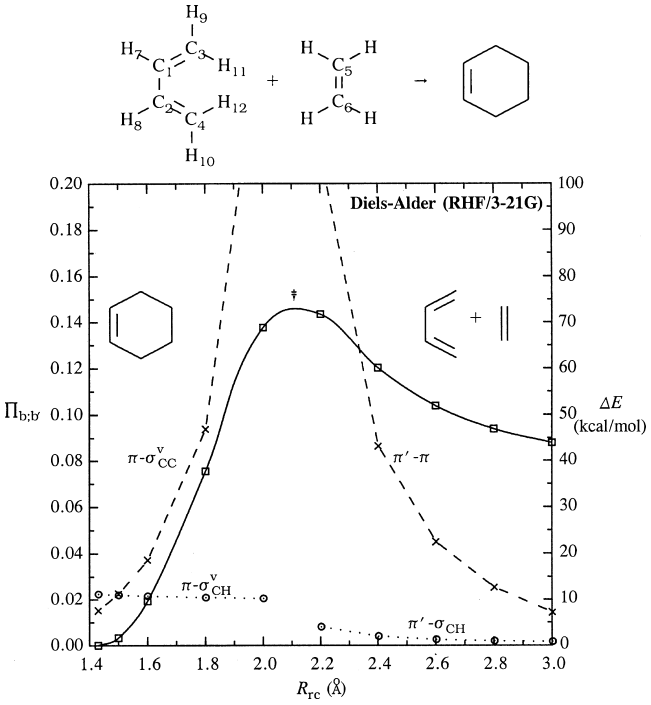

Figure 5. Intra- and intermolecular bond–bond polarizability indices for model Diels–Alder reaction (RHF/3-21G level, reaction coordinate R_{rc} = distance between C_3–C_4 and C_5–C_6 midpoints). For R_{rc} < 2.1 Å (where the product cyclohexene NBO Lewis structure is preferred), the figure shows *intra*molecular NBBP elements between the C_1–C_2 π bond and the vicinal σ CC bonds (e.g., C_3–C_5, dashed line; labeled π–σ^{v}_{CC}) or CH bonds (e.g., C_3H_{11}, dotted line; labeled π–σ^{v}_{CH}) of cyclohexene. For R_{rc} > 2.1 Å (where the optimal NBO Lewis structure corresponds to ethylene + butadiene reactant species), the figure shows the strong *inter*molecular elements between ethylene (π') and diene (π) π bonds (dashed line; labeled π'–π), as well as the much weaker interactions between π' and proximal σ_{CH} bonds (e.g., C_3–H_{11}, dotted line; labeled π'–σ_{CH}). The corresponding energy profile $\Delta E(R_{rc})$ (solid curve; right-hand scale) is plotted for values of the reaction coordinate from 3.00 Å (weakly interacting reactants) to 1.43 Å (equilibrium cyclohexene product), showing the transition state maximum near $R_{rc}^{\ddagger}$ = 2.09 Å.

For comparison, we plot on the left (product) side of the diagram the leading *intra*molecular $\Pi_{b;b'}$ elements for the product cyclohexene NBO Lewis structure, particularly the π–σ^{v}_{CC} interaction of the π bond with the vicinal CC σ bonds that are destroyed in the retro-Diels–Alder reaction. It is evident from comparison of left and right sides of this diagram that intra- and intermolecular π-delocalization effects are of *comparable* magnitude in this case, each increasing exponentially in the approach to the transition state from product or reactant directions, respectively. The example illustrates how NBBP indices provide unified comparisons of π conjugative effects for both intra- and intermolecular variations of nuclear geometry, all beyond the scope of the simple Hückel framework.

Intermolecular σ Delocalization in the Water Dimer. As a final example, we show NBBP values for the formation of a model hydrogen-bonded $(H_2O)_2$ complex (RHF/6-31+G* level), as displayed in Figure 6. In this idealized model, each monomer is assigned a fixed geometry (R_{OH} = 0.96 Å, θ_{HOH} = 105°) with idealized linear O′···H–O H-bond geometry (as shown in the figure inset) and with H_2O' tilt angle optimized at each point on the $R_{O'\cdots H}$ reaction coordinate. Such a frozen

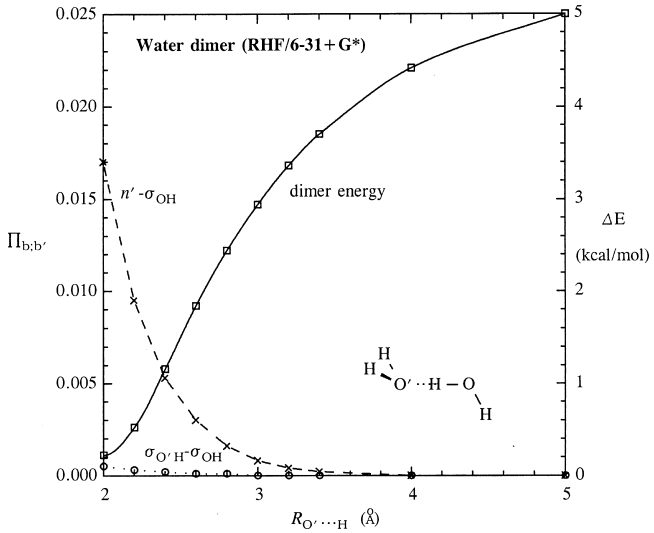

Figure 6. Intermolecular bond–bond polarizability values for model water dimer (RHF/6-31+G* level; see text), showing the strong increase of intermolecular n'–σ_{OH} conjugation (dashed line) and weaker increase of $\sigma_{O'H}$–σ_{OH} conjugation (dotted line) associated with formation of the equilbrium hydrogen bond. (n' is the O′ lone pair aligned along the linear O′···H–O H-bond axis). The relative dimer potential energy ΔE (solid line; right-hand ordinate) is shown for comparison.

monomer calculation neglects minor details of geometry relaxation but includes all significant electronic features found at higher levels.

Figure 6 exhibits the dramatic increase in $\Pi_{n(O');\sigma(OH)}$ as the hydrogen bond forms, reflecting the intermolecular delocalization (charge transfer) associated with H-bond formation. This delocalization first becomes appreciable as the reaction coordinate approaches the van der Waals contact distance (~2.8 Å), then rises exponentially as the monomers approach their equilibrium H-bonding distance (~2.0 Å at this basis level). By comparison, the next most important intermolecular NBBP element ($\Pi_{\sigma(O'H);\sigma(OH)}$) is essentially negligible.

Comparison of Figures 5 and 6 suggests the marked parallels between π delocalization in Diels–Alder adduct formation and σ delocalization in H-bond formation. Both reflect conjugative-type donor–acceptor interactions in supramolecular complex formation, although the magnitudes differ characteristically. The rapid increase of $\Pi_{n(O');\sigma(OH)}$ as the monomers penetrate van der Waals contact distance is in accord with the general NBO picture of the hyperconjugative origin of hydrogen bonding.[29]

■ SUMMARY AND CONCLUSIONS

The examples above have been chosen to exhibit the magnitudes and variations of ab initio NBBP values in prototype cases, illustrating the comparisons of conjugative (π–π) and hyperconjugative (π–σ or σ–σ) delocalization effects in a variety of intra- and intermolecular interactions. The results establish that the ab initio NBBP index maintains reasonable qualitative resemblance to its elementary Hückel-theoretic counterpart, but with considerable additional quantitative detail to describe geometry variations and more subtle forms of conjugation.

The NBBP index offers the attractive ability to identify *localized bond* regions of the molecule that are selectively affected by perturbing other bond regions by chemical

dx.doi.org/10.1021/jo301620k | J. Org. Chem. 2013, 78, 1844–1850

substitution, geometry distortions, photochemical excitation, or other means. It may thereby serve to identify specific localized structural features that prove useful in engineering desired molecular properties or reaction pathways, but are not fully apparent in the delocalized MO wave function itself.

APPENDIX: RELATION TO NBO INTERACTION ENERGIES

The bond−bond polarizability element $\Pi_{rs;tu}$ can be evaluated in limiting cases of noninteracting or weakly interacting bonds r−s, t−u. For convenience we consider the case of σ bonds (σ_{rs}, σ_{tu}), but generalizations are readily obtained for NBOs of π symmetry.

We begin by expanding the localized σ_{rs}, σ_{tu} bonds as linear combinations of natural hybrid orbitals h_r, h_s

$$\sigma_{rs} = a_r h_r + a_s h_s \tag{A1a}$$

$$\sigma_{tu} = a_t h_t + a_u h_u \tag{A1b}$$

with corresponding antibonds

$$\sigma^*_{rs} = a_s h_r - a_r h_s \tag{A2a}$$

$$\sigma^*_{tu} = a_u h_t - a_t h_u \tag{A2b}$$

Let $\Pi_{rs;tu}^{(jk)}$ denote the term of the general bond−bond polarizability expression eq 1 for occupied MO φ_j and virtual MO φ_k. In the absence of interactions between σ_{rs} and σ_{tu} bonding regions, the MOs are completely localized (say, $\varphi_j = \sigma_{rs}$, $\varphi_k = \sigma^*_{tu}$) and $\Pi_{rs;tu}^{(jk)}$ is vanishing. Similarly, if the occupied φ_j is a mixture of two or more bonds (say, φ_j = linear combination of σ_{rs}, σ_{tu}) but the virtual φ_k is localized (say, $\varphi_k = \sigma^*_{tu}$), or conversely, if φ_k is a mixture of antibonds but φ_j is localized, then $\Pi_{rs;tu} = 0$. Non-zero values of $\Pi_{rs;tu}^{(jk)}$ can therefore occur only when a bond σ_{rs} is mixed with an antibond σ^*_{tu} in *both* an occupied φ_j and virtual φ_k. Thus, $\Pi_{rs;tu}$ should be related to the strength of $\sigma_{rs}\rightarrow\sigma^*_{tu}$ and $\sigma_{tu}\rightarrow\sigma^*_{rs}$ donor−acceptor interactions between the r−s and t−u bonding regions.

Let us consider the simplest type of delocalized mixing that can lead to nonvanishing $\Pi_{rs;tu}^{(jk)}$. In the case of 2 × 2 mixing (corresponding to $\sigma_{rs} \rightarrow \sigma^*_{tu}$ delocalization, in NBO language), the MOs can be written as

$$\varphi_j = (1 - \lambda^2)^{1/2}\sigma_{rs} + \lambda\sigma^*_{tu} \tag{A2b}$$

$$\varphi_k = (1 - \lambda^2)^{1/2}\sigma^*_{tu} - \lambda\sigma_{rs} \tag{A3b}$$

where the mixing coefficient λ expresses the strength of σ_{rs}−σ^*_{tu} interaction. In this case it is easy to verify that $\Pi_{rs;tu}^{(jk)}$ reduces to

$$\Pi_{rs;tu}^{(jk)} = 8\lambda^2(1 - \lambda^2)a_r a_s a_t a_u/(\varepsilon_k - \varepsilon_j) \tag{A4}$$

In leading order of NBO perturbation theory, the mixing coefficient λ in (A3) can be approximated as

$$\lambda = F_{\sigma\sigma^*}/(F_{\sigma^*\sigma^*} - F_{\sigma\sigma}) \tag{A5}$$

where $F_{\sigma\sigma}$, $F_{\sigma\sigma^*}$, $F_{\sigma^*\sigma^*}$ are Fock matrix elements for σ (= σ_{rs}) and σ^* (= σ^*_{tu}) NBOs. In terms of the usual second-order NBO estimate $\Delta E^{(2)}_{\sigma\sigma^*}$ of σ−σ^* interaction energy

$$\Delta E^{(2)}_{\sigma\sigma^*} = 2F_{\sigma\sigma^*}{}^2/(F_{\sigma^*\sigma^*} - F_{\sigma\sigma}) \tag{A6}$$

Equation A4 can therefore be rewritten finally as

$$\Pi_{rs;tu}^{(jk)} = [4a_r a_s a_t a_u/(F_{\sigma^*\sigma^*} - F_{\sigma\sigma})^2]\Delta E^{(2)}_{\sigma\sigma^*} \tag{A7}$$

where $\sigma = \sigma_{rs}$, $\sigma^* = \sigma^*_{tu}$.

In the elementary case of homopolar bonds ($a_r = a_s = a_t = a_u = 2^{-1/2}$), the numerator of the bracketed prefactor in A7 reduces to unity. Its value would tend to remain of order unity for more general polar covalent bonds (as determined by atomic electronegativity differences) . In atomic units, the energy difference ($F_{\sigma^*\sigma^*} - F_{\sigma\sigma}$) in the denominator also tends to be of order unity. In ethylene, for example, this denominator is 1.91 au for a CC σ bond or 0.60 au for the corresponding CC π bond. In the absence of direct bond-breaking processes (which affect $F_{\sigma^*\sigma^*}$, $F_{\sigma\sigma}$ strongly), the factors preceding $\Delta E^{(2)}_{\sigma\sigma^*}$ in eq A7 are therefore relatively constant and of order unity, which establishes the approximate proportionality relationship in text eq 6.

AUTHOR INFORMATION

Corresponding Author

*E-mail: weinhold@chem.wisc.edu.

Notes

The authors declare no competing financial interest.

†Deceased.

ACKNOWLEDGMENTS

The original draft of this article was prepared to amplify on refs 4 and 6 of the initial NBBP communication[8] with more methodical theoretical and numerical documentation of the NBBP program module that entered the NBO program. However, the press of NBBP applications to other problems nudged such documentation ever backward on the proverbial burner. This special memorial issue presents the opportunity to update and complete the intended collaborative work, which well reflects H.E.Z.'s special enthusiasm for tracing the surprising Hückel-like patterns of chemical behavior to deeper quantum mechanical origins.

REFERENCES

(1) Coulson, A. A.; Longuet-Higgins, H. C. *Proc. R. Soc. London, Ser. A* **1947**, *191*, 39−60; **1947**, *192*, 16−32.

(2) For general discussions of bond−bond polarizabilities in the Hückel framework, see: Streitwieser, A. *Molecular Orbital Theory for Organic Chemists*; John Wiley: New York, 1961; p 107ff. Salem, L. *Molecular Orbital Theory of Conjugated Systems*; Benjamin: New York, 1966; pp 35, 148−152. Daudel, R.; Lefebvre, R.; Moser, C. *Quantum Chemistry, Methods and Applications*; Interscience: New York, 1959; pp 80−83.

(3) Chirgwin, B. H.; Coulson, C. A. *Proc. R. Soc. London, Ser. A* **1950**, *291*, 196−209.

(4) McWeeny, R., Löwdin, P.-O. Pullman, B. In *Molecular Orbitals in Chemistry, Physics, and Biology: A Tribute to R. S. Mulliken*; Academic Press: New York, 1964; pp 305−328.

(5) Greenwood, H. H.; Hayward, T. H. *Mol. Phys.* **1960**, *3*, 495−509.

(6) Pople, J. A.; D. P. Santry, D. P. *Mol. Phys.* **1964**, *8*, 1−18.

(7) Foster, J. P.; Weinhold, F. *J. Am. Chem. Soc.* **1980**, *102*, 7211−7218. Reed, A. E.; Weinstock, R. B; Weinhold, F. *J. Chem. Phys.* **1985**, *83*, 735−746. For a current overview, see: Weinhold, F.; Landis, C. R. *Discovering Chemistry with Natural Bond Orbitals*; Wiley: Hoboken, NJ, 2012.

(8) Zimmerman, H. E.; Weinhold, F. *J. Am. Chem. Soc.* **1994**, *116*, 1579−1580.

(9) Liang, C. X.; Newton, M. D. *J. Phys. Chem.* **1992**, *96*, 2855−2866. Jordan, K. D.; Paddon-Row, M. N. *Chem. Rev.* **1992**, *92*, 395−410. Curtiss, L. A.; Naleway, C. A.; Miller, J. R. *J. Phys. Chem.* **1995**, *99*, 1182−1193. Paddon-Row, M. N.; Shephard, M. J. *J. Am. Chem. Soc.*

1997, *119*, 5355−5365. Paddon-Row, M. N. *Adv. Phys. Org. Chem.* **2003**, *38*, 1−85. Goldsmith, R. H.; Vura-Weis, J.; Scott, A. M.; Borkar, S.; Sen, A.; Ratner, M. A.; Wasielewski, M. R. *J. Am. Chem. Soc.* **2008**, *130*, 7659−7669. Nishioka, H.; Ando, K. *Phys. Chem. Chem. Phys.* **2011**, *13*, 7043−7059.

(10) Zhou, P.; Ayers, P. W.; Lu, S.; Li, T. *Phys. Chem. Chem. Phys.* **2012**, *14*, 9890−9896.

(11) Kim, W. K.; Sohn, C. K.; Linn, S. H.; Rhee, S. K.; Kim, C. K.; Lee, I. *Bull. Korean Chem. Soc.* **1999**, *20*, 1177−1188. Sengar, R. S.; Nemykin, V. N.; Basu, P. *New J. Chem.* **2003**, *27*, 1115−1123. Düfert, A.; Werz, D. B. *J. Org. Chem.* **2008**, *73*, 5514−5519. Hodges, A. A.; Raines, R. R. *Org. Lett.* **2008**, *8*, 4695−4697. Xiao-Hong, L.; Zheng-Xin, T.; Xian-Zhou, Z. *Int. J. Quantum Chem.* **2010**, *110*, 1565−1572. Oziminski, W. P.; Krygowski, T. M. *J. Mol. Mod.* **2011**, *17*, 565−572.

(12) Sadlej-Sosnowska, N. *J. Org. Chem.* **2001**, *66*, 8737−8743. Norton, J. E.; Briseno, A. L.; Wudl, F.; Houk, K. N. *J. Phys. Chem. A* **2006**, *17*, 9887−9899. Liu, S.-B.; Pedersen, L. G. *J. Phys. Chem. A* **2009**, *113*, 3648−3655. Limacher, P. A.; Lüthi, H.-P. *WIREs Comp. Mol. Sci.* **2011**, *1*, 477−486.

(13) *Gaussian 92*: Frisch, M. J.; Trucks, G. W.; Head-Gordon, M.; Gill, P. M. W.;Wong, M. W.; Foresman, J. B.; Johnson, B. G.; Schlegel, H. B.; Robb, M. A.; Replogle, E. S.; Gomperts, R.; Andres, J. L.; Raghavachari, K.; Binkley, J. S.; Gonzalez, C.; Martin, R. L.; Fox, D. J.; Defrees, D. J.; Baker, J.; Stewart, J. J. P.; Pople, J. A. Gaussian, Inc.: Pittsburgh, PA, 1992.

(14) *NBO 5.0*: Glendening, E. D.; Badenhoop, J. K.; Reed, A. E.; Carpenter, J. E.; Bohmann, J. A.; Morales, C. M.; Weinhold, F. Theoretical Chemistry Institute, University of Wisconsin: Madison, WI, 2001; http://www.chem.wisc.edu/~nbo5 (accessed July 29, 2012). Discussion of "sign-corrected" $\Pi_{rs;tu}$ values (correcting for choices of coordinate system that reverse hybrid phase and apparent sign of β) is given in the *NBO 5.0 Manual*.

(15) For standard ab initio computational methods and basis set designations used herein, see: Foresman, J. B.; Frisch, A. E. *Exploring Chemistry with Electronic Structure Methods*, 2nd ed.; Gaussian Inc.: Pittsburgh, PA, 1996.

(16) Pople, J. A.; Gordon, M. *J. Am. Chem. Soc.* **1967**, *89*, 4253−4261.

(17) For discussion of the relationship between NBOs and PNBOs (visualization orbitals), see: Weinhold, F.; Landis, C. R. *Discovering Chemistry with Natural Bond Orbitals*; Wiley: Hoboken, NJ, 2012; p 35, 38, 98−99; http://www.chem.wisc.edu/~nbo5/web_nbo.htm (accessed July 29, 2012).

(18) For discussion of superficial aspects of canonical MO "delocalization", see: Weinhold, F., Natural bond orbital analysis: A critical overview of relationships to alternative bonding perspectives. *J. Comput. Chem.* **2012**, DOI: 10.1002/jcc.23060 http://www.chem.wisc.edu/~nbo5/cmo.htm (accessed July 29, 2012).

(19) Mulliken, R. S. *J. Chem. Phys.* **1939**, *7*, 339−352.

(20) Schleyer, P. v.R.; Kos, A. J. *Tetrahedron* **1983**, *39*, 1141−1150.

(21) Alabugin, I. V.; Gilmore, K. M.; Peterson, P. W. *WIREs Comp. Mol. Sci.* **2011**, *1*, 109−141.

(22) Hoffmann, R. *Acc. Chem. Res.* **1971**, *4*, 1−9 , ref 9.

(23) Deslongchamps, P. *Stereoelectronic Effects in Organic Chemistry*; Pergamon: New York, 1983.

(24) Brunck, T. K.; Weinhold, F. *J. Am. Chem. Soc.* **1979**, *101*, 1700−1709. Reed, A. E.; Weinhold, F. *Isr. J. Chem.* **1991**, *31*, 277−285. Weinhold, F. *Nature* **2001**, *411*, 539−541.

(25) Although RHF is a sufficient zeroth-order description for this simple Woodward−Hoffmann-allowed model reaction, more general bond-breaking processes require unrestricted UHF (or higher multireference) description. In the open-shell UHF case, distinct NBBP indices are calculated for each spin set and composite $\Pi_{rs;tu}$ is a spin-averaged sum of α-NBBP and β-NBBP contributions for the chosen nuclear centers (cf. ref 14).

(26) For the corresponding reaction of butadiene with 1,2-difluoroethylene (which occurs at an experimentally useful rate), we find at the same RHF/3-21G level a weak attractive well in the entrance channel (−1.9 kcal/mol at R_{rc} = 3.0Å) and additional significant $\Pi_{b;b'}$ interactions between fluorine lone pairs and the hexene π bond. However, in other respects the results are qualitatively similar to those shown in Figure 5.

(27) The precise mathematical nature of the divergent behavior has not been quantified, but presumably involves both rapid increase of exchange-type hybrid interaction coefficients in the numerator and increasingly singular near-degeneracy in the denominator of eq 1.

(28) Fleming, I. *Frontier Orbitals and Organic Chemical Reactions*; Wiley: New York, 1976.

(29) Reed, A. E.; Curtiss, L. A.; Weinhold, F. *Chem. Rev.* **1988**, *88*, 899−926. Weinhold, F. *Adv. Protein Chem.* **2008**, *72*, 121. Weinhold, F.; Klein, R. A. *Mol. Phys.* **2012**, *110*, 565−579.